Unraveling assemblage of microbial community dwelling in Dabaoshan As/Pb/Zn mine-impacted area: A typical mountain mining area of South China

Jian-Li Liu, Jun Yao, Ruofei Li, Houquan Liu, Jun-Jie Zhu, Geoffrey Sunahara, Robert Duran

Unraveling assemblage of microbial community dwelling in Dabaoshan As/Pb/Zn mine-impacted area: A typical mountain mining area of South China

Jian-li Liu [a *], Jun Yao [a], Ruofei Li [a], Houquan Liu [a], Jun-jie Zhu [a], Geoffrey Sunahara [a,b], Robert Duran [a,c]

[a] School of Water Resources and Environment and Research Center of Environmental Science and Engineering, Sino-Hungarian Joint Laboratory of Environmental Science and Health, Beijing Key Laboratory of Water Resources & Environmental Engineering, China University of Geosciences (Beijing), 29 Xueyuan Road, Haidian District, 100083 Beijing, China

[b] Department of Natural Resource Sciences, McGill University, Montreal, Quebec, H9X3V9, Canada

[c] Université de Pau et des Pays de l'Adour/E2S UPPA, IPREM UMR CNRS 5254, BP 1155, 64013 Pau Cedex, France

Submitted to: ***Science of the Total Environment***

Word count: 4910 (excluding Abstract, References, and figure and table captions)

Figures: 6

* Corresponding Author. School of Water Resource and Environment Engineering, China University of Geosciences (Beijing), 29 Xueyuan Road, Haidian District, 100083 Beijing, China, E-mail: ljl2489@cugb.edu.cn (J. Yao), Tel: +86-10-82321958

Abstract

Microbial community assemblage includes microorganisms from the three domains including Bacteria, Archaea, and Eukarya (Fungi), which play a crucial role in geochemical cycles of metal(loid)s in mine tailings. Mine tailings harbor vast proportions of metal(loid)s, representing a unique source of co-contamination of metal(loid)s that threaten the environment. The elucidation of the assembly patterns of microbial communities in mining-impacted ecospheres has received little attention. To decipher the microbial community assembly processes, the microbial communities from the five sites of the Dabaoshan mine-impacted area were profiled by the MiSeq sequencing of 16S rRNA (Bacteria and Archaea) genes and internal transcribed spacers (Fungi). Results indicated that the coexistence of 31 bacterial, 10 fungal, and 3 archaeal phyla, were mainly dominated by *Mucilaginibacter*, *Cladophialophora*, and *Candidatus Nitrosotalea*, respectively. The distribution of microorganisms was controlled by deterministic processes. The combination of Cu, Pb, and Sb was the main factor explaining the structure of microbial communities. Functional predicting analysis of bacteria and archaea based on the phylogenetic investigation of communities by reconstruction of unobserved states analyses revealed that the metabolic pathways related to arsenite transporter, arsenate reductase, and Fe-S cluster were important for metal detoxification. Furthermore, the ecological guilds (pathogens, symbiotrophs, and saprotrophs) of fungal communities explained 44.5% of functional prediction. In addition, metal-induced oxidative stress may be alleviated by antioxidant enzymes of fungi communities, such as catalase. Such information provides new insights into the microbial assembly rules in co-contaminated sites.

Keywords: Assembly process; Mine-impacted ecospheres; Co-occurrence network; Potential functional metabolism; Keystone taxa

1. Introduction

Sustainable environmental protection for non-ferrous mining wastes is vital for the development of the national economy, industry, science, and technology. The annual discharge of non-ferrous mining and smelting slag in the world exceeds 10 billion tons, which are open-air stacked in mine tailing dams (Wang *et al.*, 2017). The content of metal(loid)s in non-ferrous tailings accounts for 30% - 90% of total industrial discharges, and flotation reagents were three times more enriched than pesticides in agricultural fields (Liu *et al.*, 2018; Zhang *et al.*, 2020). Such large quantities of tailings containing toxic, hardly decomposed, and complex multiple contaminants have seriously threatened food security and ecological security (Alakangas *et al.*, 2010; Liu *et al.*, 2022a; Zhu *et al.*, 2018). Complexation between metals and organic flotation reagents can accelerate the migration and transformation of metals, as well as inhibit the degradation of flotation reagents (Zhang *et al.*, 2020; Zhu *et al.*, 2018). Furthermore, exposure to toxicants in anthropogenic tailing dams by drinking the contaminated water, ingestions of soil and food grown on the waste, and dust inhalation could lead to dire consequences for human health (Hudson-Edwards, 2016; Torres *et al.*, 2018; Wang *et al.*, 2017).

Arsenic (As) bearing minerals are ubiquitous in tailings, including sulfides, sulfosalts, arsenates, and arsenites (Giloteaux *et al.*, 2013). Arsenic has been listed as a suspected carcinogen by the International Agency for Research on Cancer, which is an agency of the World Health Organization. Additionally, the United States Environmental Protection Agency and the United Nations Environment Programme also recognize arsenic as a hazardous substance with potential carcinogenic properties. Arsenic, regarded as an environmental threat for all types of organisms, could induce cancers of the skin, lung, liver, and bladder among other tissues (Speer *et al.*, 2023).

Besides arsenic, elevated concentrations of associated metal(loid)s, such as copper (Cu), lead (Pb), and zinc (Zn), are frequently found in or around mine tailings worldwide (Hudson-Edwards, 2016).

Microorganisms (including Bacteria, Archaea, and Fungi) are important in the transformation of metal(loid)s ensuring the functions that sustain ecosystems. Bacteria are the dominant tailing-associated microorganisms (> 97%), followed by Archaea (0.26% - 2.75%), and Eukarya (0.21% - 0.11%) (Liu *et al.*, 2023). The distribution and composition of microorganisms can be driven by the spatial-temporal heterogeneity of geochemical factors, climate, and temperature (Liang *et al.*, 2020; Yi *et al.*, 2022). However, most studies have only focused on a single microbial component, i.e., bacteria (Liu *et al.*, 2019a; Sun *et al.*, 2018), fungi (Liu *et al.*, 2022b; Suting and Olivia Devi, 2021), or archaea (Chen *et al.*, 2021; Mendez-Garcia *et al.*, 2015). Bacterial, fungal, and archaeal communities can contribute to the transformation of metal(loid) speciations and the degradation of flotation reagents in the co-contamination nonferrous mine environment. Intrinsic linkages between assembly processes and co-occurrences of bacteria, fungi, and archaea could facilitate the management of microorganisms for better provision of ecosystem services. However, to our knowledge, the co-occurrence of overall microbial assemblages including bacterial, fungal, and archaeal communities in tailings has not been well investigated.

To address this research gap, a study was conducted at a nonferrous mine tailing site with As/Pb/Zn co-contaminated in a Dabaoshan mine-impacted area (see Supplementary Information Fig. S1 and Table S1). We hypothesize here that: (1) the assembly processes of bacterial, fungal, and archaeal communities are influenced by various factors, including both biotic and abiotic elements, and (2) microbiological

communities with lower levels of species richness show greater linkages between species. We analyzed the samples collected from the Dabaoshan As/Pb/Zn mine-impacted area in a typical mountain mining area of South China. The objectives of this study were to (1) evaluate the diversity, structure, and composition of bacterial, fungal, and archaeal taxa in tailings; (2) reveal the ecological assembly processes and co-occurrence patterns of the three domain taxa under the long-term metal(loid)s co-contamination; and (3) explore the potential functional metabolism of taxa, which could be used for the management of microbial resources. This study provides new insights for studying community ecology, predicting responses to environmental changes, and designing strategies for microorganism management and site restoration.

2. Materials and methods

2.1 Site description, sampling, and physical-chemical analyses

The Dabaoshan mining area is located in the northern Guangdong province (southern China) and Lingnan mountain region with a hilly landform (24°30′01″ - 24°35′26″ N, 113°41′53″ - 113°46′40″ E, Fig. S1). The Dabaoshan mine, a typical mountainous mining area, is the largest in South China (Wang *et al.*, 2019). It is a large polymetallic mine composed mainly of Fe and Cu. It has been mined extensively since the 1970s, and most of the metal ores are S-containing ores such as pyrite, pyrrhotite, and chalcopyrite, which are important for the generation of acid mine drainage (Bao *et al.*, 2018). The upper part of the polymetallic deposit was a weathered and leached limonite, the middle part was layered siderite, and the lower part was Cu, Pb, Zn, Fe, and S deposits, and porphyry Mb and Mb polymetallic deposits (Luo *et al.*, 2021). The tailings site had been used for open storage of Pb-Zn or Fe smelting slag for almost 30 years and was abandoned for almost 20 years. The total amount of various solid wastes is over 9 million tons.

126 The sampling area covers a total surface area of 0.47 ha (Fig. S1). This area was
127 selected based on previous physical-chemical characterization studies (Zhang *et al.*,
128 2019), and has been undergoing natural attenuation for almost 20 years. The sampling
129 area was divided into five general sub-areas, which were divided along the directions
130 of the surrounding LiWu river (Fig. S1) and showed different physical-chemical
131 properties characteristics (Table S1). Due to the irregular terrain with high
132 heterogeneity of tailings, a random sampling strategy was adopted collecting
133 composite samples by nested sampling within a site. Composite samples using a
134 nested sampling design within a site accounted for environmental heterogeneity and
135 were reasonably reliable for the evaluation of the microbial diversity variation at a
136 small scale (Liu *et al.*, 2019).

137 For each sub-area, 13 samples were collected in December 2021 based on a
138 squared-figure sampling design. Samples were then combined and homogenized to
139 produce a composite sample to evaluate variations of bacteria, fungi, and archaea
140 communities. A total of five composite samples were finally harvested after field
141 sampling. All composite samples were immediately kept on ice (at 4°C) and delivered
142 to the China University of Geosciences (Beijing) within 48 h of sampling. Samples
143 for physical-chemical analysis were air-dried and sieved at 100-mesh size (0.149 mm,
144 US standard).

145 The detection of pH was done following the procedure of the China National
146 Agricultural Technology Extension Center (2006). After digestion in a microwave
147 with HNO_3-HCl-HF (5:3:2, v/v/v, GR), the concentrations of metal(loid)s were
148 measured by inductively coupled plasma-mass spectrometry (ICP-MS). More detailed
149 information for the measurements of pH and metal(loid)s concentrations was
150 previously described by Liu *et al.* (2021). The mineralogical composition of the

sample was determined using a scanning electron microscope (SEM) and energy dispersive spectroscopy (EDS) spectrometer analysis, combined with phase analysis of X-ray diffraction (XRD) and X-ray fluorescence (XRF). For microorganism analysis, samples from each site were stored at -80 ℃ for further DNA extraction and Miseq sequencing.

2.2 Amplification, MiSeq sequencing, and data processing

Total genomic DNA was extracted from ~ 10.0 g of each tailing sample using a FastDNA® spin kit for soil (MP, Biomedicals, USA). The extracted DNA was subjected to PCR amplification using the primer sets of: 1) ArBa515F (GTGCCAGCMGCCGCGGTAA) and 806R (GGACTACHVGGGTWTCTAAT), targeting the V3-V4 region of bacterial 16S rRNA gene (Liu *et al.*, 2023); 2) ITS1-F (CTTGGTCATTTAGAGGAAGTAA) and ITS2-R (GCTGCGTTCTTCATCGATGC), targeting the fungal genomic ITS region (Liu *et al.*, 2022c); 3) 524F10extF (TGYCAGCCGCCGCGGTAA) and Arch958RmodR (YCCGGCGTTGAVTCCAATT), targeting the V3-V4 region of archaeal genomic gene (Yi *et al.*, 2019). Polymerase chain reaction (PCR) reaction (20 μL) was carried out containing 10 μL of 2×Pro Taq, 0.8 μL of forward/reverse primers (5 μM), 10 ng/μL of extracted template DNA, and double-distilled water. The PCR reaction was performed on an ABI GeneAmp® 9700 Thermal Cycler with the procedures: initial denaturation (3 min at 95°C), followed by 27 cycles of 30 s at 95°C, annealing 30 s (at 55°C for bacteria, 55°C for archaea, and 50°C for fungi), and extension (45 s at 72°C), and a final extension (10 min at 72°C). This reaction was carried out (in triplicate) for each composite sample, and then these samples were mixed into a new PCR composite sample for sequencing. Sequencing was conducted on an Illumina MiSeq platform at Majorbio Bio-Pharm Technology Co., Ltd (Shanghai, China).

The acquired sequences were filtered, and chimeric sequences were removed using the USEARCH7-uparse clustering algorithm. Sequences were then split into operational taxonomic units (OTUs) at a 97% similarity level according to 70% classification confidence as previously described (Mamet *et al.,* 2017; Liu *et al.*, 2019a). All raw data were trimmed and filtered using fastp software (v0.19.4) by filtering the reads below 50bp and reads with nitrogenous base. The fast length adjustment of short reads (FLASH) software was used for merging the paired-end reads of raw sequences. Sequences of bacterial/archaeal, and fungal were assigned to taxonomic based on the taxonomy database of silva138/16s and unite8.0/its_fungi, respectively. The sequence read archive accession number for the sequences is SUB13926409.

2.4 Statistical analyses

To determine the differences in alpha-diversities of bacterial, fungal, and archaeal communities, analyses based on the Wilcoxon test were calculated using OTUs tables resampled to a minimum number of sequences from each sample (39,922 for bacteria, 72,629 for fungi, and 42,962 for archaea). In present study, $p < 0.05$ is considered statistically significant. To estimate the beta-diversity of bacterial, fungal, and archaeal communities, non-metric multidimensional scaling (NMDS) was conducted based on the Bray-Curtis dissimilarity algorithms. The Partial Mantel test determined the correlations between compositional and environmental data based on Euclidean distances (Sunagawa *et al.*, 2015). BIOENV analysis was used to determine the combined effects of physical-chemical parameters on the distribution of microbial communities. The incidence-based (Raup-Crick) dissimilarity indices (β_{RC}) were computed to determine whether communities were stochastically or deterministically assembled. The neutral community model was constructed to evaluate the

contribution of neutral processes in community structure as described by others (Sloan *et al.*, 2006). The Levins' niche breadth index for meta-communities was estimated to reveal the patterns of meta-communities sorting and dispersal limitation and their adaptability to the contaminated tailings. A high breadth index for a given community indicates its wide habitat niche breadth. The wider the species niche, the species is less specialized and more metabolically flexible. Co-occurrence network analyses of bacterial, fungal, and archaeal communities were conducted by Gephi software (v0.9.2) using the Frucherman Reingold algorithm as described by others (Han *et al.*, 2017). The degree of the node of the co-occurrence network was assessed by the number of nodes connected directly to that node. The more lines on the node, the higher the degree, which indicates the intensity of correlation between the species and other species.

To predict the potential functions of bacterial and archaeal communities, the Phylogenetic Investigation of Communities by Reconstruction of Unobserved States (PICRUSt2) was used to reveal the functions encoded in communities based on the MetaCyc database. The weighted nearest sequenced taxon index (NSTI) was calculated to assess the accuracy of PICRUSt2 analysis (Langille *et al.*, 2013). Kyoto Encyclopedia of Genes and Genomes (KEGG) databases (e-value cut-off 10^{-5}) were used for functional annotation. Significant differences in KOs between bacterial and archaeal communities were analyzed based on the independent samples *T*-test. To identify different functional groups within fungal communities, a recently developed open annotation tool (FunGuild, Fungi Functional Guild) was used for the assignment of fungal communities (Nguyen *et al.*, 2016). Redundancy analysis was used to examine the correlations between KOs/Guilds and physical-chemical parameters based on a weighted normalized unifrac distance algorithm. All the analyses were

done using R software (v 3.4.1) unless otherwise stated.

3. Results and discussion

3.1 The morphological characteristics of main mineral grains

The pH in the five studied samples ranged from 4.03 to 6.56 (Table S1), being higher than the reported abandoned tailings (Liu *et al.*, 2019b; Liu *et al.*, 2021). Generally, the heavy mineral fractions have typical metal(loid) concentrations that are one order of magnitude greater, indicating that the majority of the contaminants are likely bonded to high-density phases (Tuhý *et al.*, 2020). The metal(loid) concentration (mg/kg) in the mineral fractions were in the following ranges: As (from 2180 to 2810), Fe (72900 - 97900), Pb (2800 - 4060), and Zn (1260 – 2220) (Table S1). The levels of As, Fe, Pb, and Zn were from 1.36 to 17.98 times higher than the soil environmental quality standard (GB15628-1995 and GB36600-2018). Presumably, this contamination followed the release of metal(loid)s from smelter tailing after > 30 years of abandonment (Alakangas *et al.*, 2010). According to the ICP-MS analysis, the major potential toxicants were As, Pb, and Zn, resulting in metal(loid) pollution in the Dabaoshan mine-impacted area. Correlation analysis between metal(loid)s showed that As, Pb, Sb, and Zn had a significant positive correlation with each other (r = 0.878 - 0.978; $p < 0.05$ or $p < 0.01$; Table S2) in the studied sites. As well, Cr had a high correlation coefficient with Cu (r = 0.916; $p <$ 0.05; Table S2). Results suggested that the elements had the same source, with similar physical-chemical properties.

The XRD analysis indicated that samples were predominantly composed of quartz, manganese copper oxide, Iwakiite, Celadonite, and Magnesium iron oxide (Fig. 1).

These five minerals, except quartz and Iwakiite, were often observed in the gangue minerals. Some very complex minerals were also present as other minor phase forms (Fig. 1). The presence of minor mineral phases may correspond to the high-temperature amorphous and nanocrystalline phases produced during the smelting and refining operations (Tuhý *et al.,* 2020; Zhu *et al.*, 2021). Representative SEM-EDS images of the typical minerals are shown in Figure 1.

< Insert Fig. 1 >

The main minerals presented as irregular large particles and were composed of various mineral grain aggregates. Moreover, the elemental composition (%) of tailings samples consisted mainly of C (from 5.35 to 33.85), O (40.33 - 61.91), P (0.28 - 1.87), Si (5.00 - 21.94), and S (0.15 - 2.11) (Table S3). The major metals were Al (6.21 - 17.84), As (0.11 - 1.36), Fe (1.00 - 38.96), Pb (0.16 - 4.47), and Zn (0.09 - 1.61), as confirmed by XRF analysis (Table S4). It is likely that As and Zn participated in the silicate structure (Zhu *et al.*, 2021). These results differed from data from samples collected from Namibian mining/smelting-polluted soils (Tuhý *et al.,* 2020). Such different mineral structures are probably due to different mining/smelting processes adapted to the ore grade and the target extracted metals (Alakangas *et al.*, 2010; Liu *et al.*, 2019a,2020; Tuhý *et al.*, 2020).

3.2 Characteristics of microbial communities

A total of 31 bacterial (1042 OTUs), 10 fungal (328 OTUs), and 3 archaeal (70 OTUs) phyla were obtained, which are consistent with earlier metagenomic analyses showing that ~ 97% of microorganisms in tailings are assigned to bacteria (Liu *et al.*, 2023). The microbial diversity, relative abundance, and phylogenetic diversity following down-weighting changed as follows: bacteria, fungi, and archaea (Fig. 2a).

The boneh and coverage estimates indicated that there would be no additional observed OTUs for an additional level of sampling (coverage index > 99.87%). There were differences in alpha-diversity indices (such as Shannon, Simpson, Chao1, ace, and coverage) among bacterial, fungal, and archaeal communities ($p < 0.05$). The distributions of OTUs based on BIOENV analysis appeared strongly driven by the combination of pH, Pb, and Zn (bacteria OTUs, $r = 0.77$), Fe and Pb (fungi OTUs, $r = 0.77$), and Fe and Pb (archaea OTUs, $r = 0.37$) (Table S5). These results suggested that physical-chemical parameters influenced the distribution of the OTUs from the different microbial domains, which was consistent with other studies showing that the dynamics of physical-chemical parameters as well as their complex combinations can drive the microbial structure (Mamet *et al.*, 2017; Yi *et al.*, 2022).

< Insert Fig. 2 >

Among the 31 bacterial phyla, *Pseudomonadota* (25.3% - 38.6%), *Acidobacteriota* (0.62% - 18.3%), and *Nitrospirota* (0.16% - 23.9%) dominated the tailings sites (Fig. 2b). *Pseudomonadota* and *Acidobacteriota* are common phyla in tailings from different locations (Liu *et al.*, 2018). *Nitrospirota* includes only three valid and published genera, harboring potentially dissimilatory sulfur metabolisms (Umezawa *et al.*, 2020). In the fungal communities, *Ascomycota* and *Basidiomycota* accounted for > 95.2% of the sequences across all tailings (Fig. 2c). These fungal phyla are dominant in various environments, such as soil (Moussa *et al.*, 2017) and lead-zinc tailings (Jia *et al.*, 2021). Archaeal communities were dominated by *Thermoplasmatota* (56.6%) and *Crenarchaeota* (43.3%) phyla (Fig. 2d). Evidence showed that the *Thermoplasmatota* accounted for 75.1%, while *Crenarchaeota* were not represented in an acid mine drainage environment of France (Bruneel *et al.*, 2008; Calum 2023). This is likely due to the different geological environment conditions

299 and tailings types. *Thermoplasmatota* and *Crenarchaeota*, which harbor aerobic
300 respiration and acid tolerance genes, could contribute to the indigenous microbial
301 genetic repertoire to expand into a new habitat (Brochier-Armanet *et al.*, 2008;
302 Sheridan *et al.*, 2022). Also, there are few studies on the composition and structure of
303 the archaeal communities in metal(loid) tailings. In the present study, most of the
304 sequences could not be identified for bacteria (54.2%), fungi (26.1%), and archaea
305 (44.4%) (Fig. 2b-d). The microbial identification described here was lower than that
306 reported for other tailings such as Sb-rich or multi-contaminated nonferrous
307 metal(loid) tailings dumps (Liu *et al.*, 2019b; Xiao *et al.*, 2016). Such observation
308 suggests that a vast microbial population in tailings remains under-exploited; their
309 exploration would benefit bioremediation and environmental management (Liu *et al.*,
310 2019a).

311 3.3 Potential processes governing the microbial assemblage

312 We also explored the microorganism taxonomic classifications and their relative
313 distributions in tailings. The NMDS ordination analysis based on Bray-Curtis
314 similarity distance assessed the beta-diversity of the bacterial, fungal, archaeal, and all
315 microbial communities in tailings (Fig. 3a-d). Bacterial and fungal communities were
316 only detected in four sampling sites except at the T2 site (Fig. 2b,c), and tailing sites
317 (T3 and T5) with a pH > 5 were compared to that < pH 5 (T1 and T4) (Fig. 3a,b).

318 < Insert Fig. 3 >

319 The pH plays a critical role in affecting the abundance and distribution of microbes
320 (Chen *et al.*, 2014). Unexpectedly, archaeal communities were detected in five sites,
321 including the T2 sampling site (Fig. 2d), which was distant from the other sites (Fig.
322 3c). Also, the distribution of bacterial and fungal communities was more similar to

each other than that of archaeal communities ($p = 0.018$, stress = 0.073, permutations = 999; Fig. 3d). The environmental factors driving the relationships between the three domains of life were examined based on Mantel test (Fig. 3b). Overall, the Cu, Pb, and Sb contents were the major factors correlating with the abundance distribution of bacteria, fungi, and archaea ($p < 0.05$; Fig. 3b), whereas the pH, Fe, and Zn contents were not correlated ($p > 0.05$; Fig. 3b). Such observation probably reflects the dissimilarity distribution of OTUs among the sites, suggesting that the microbial composition exhibits habitat-specific patterns. This confirms the possibility that the distribution and composition of microbial communities are changed by dynamic and rapidly changing conditions, likely caused by anthropogenic activity-induced stresses, temperature, oxygen, salinity, latitude, and seasonal changes (Cabral *et al.*, 2016; Cravo-Laureau *et al.*, 2017; Giloteaux *et al.*, 2013; Pringault *et al.*, 2008). Nevertheless, in natural environments, the composition and distribution of microorganisms interact with both biotic and abiotic components (Cravo-Laureau *et al.*, 2017). Network analysis showing the co-occurrence abundance of members of the three domains of life indicated that *Mucilaginibacter*, *Cladophialophora*, and *Candidatus Nitrosotalea* were found as Specialists, being the main contributing genera (Fig. 4).

< Insert Fig. 4 >

It is also worth mentioning that co-occurrence analysis identified the rare taxa of *Mucilaginibacter* and *Cladophialophora* (< 1.79%; Fig. 2b,c) identified as Specialist, corresponding to keystone taxa organizing the microbial assemblage in tailings. Recent studies explored that keystone taxa have a pivotal role in driving microbial structure and functioning (Banerjee *et al.*, 2018; Herren and McMahon, 2018). Both *Mucilaginibacter* and *Cladophialophora* contain members resistant to potential toxic

348 metal(loid)s and can adapt to contaminated environments (Taleski *et al.*, 2020;
349 Vasconcelos *et al.*, 2021). Additionally, the dominated archaeal members of
350 *Candidatus Nitrosotalea* (16.2% - 70.6%; Fig. 2d) were also affiliated with keystone
351 taxa. *Candidatus Nitrosotalea*, an obligate acidophilic ammonia oxidizer, contains
352 genes encoding predicted potential pH homeostasis mechanisms (Lehtovirta-Morley
353 *et al.*, 2016). Thus, our results revealed that both rare and abundant taxa contribute to
354 ecosystem stability and function, which is consistent with previous reports in coastal
355 systems (Hugoni *et al.*, 2013).

356 To define the relative importance of deterministic and stochastic processes in
357 shaping microbial community structure incidence-based (Raup-Crick) beta-diversity
358 (β_{RC}) tests were conducted (Fig. 5a). The mean values of β_{RC} were close to |1| for the
359 three domains of life, indicating deterministic processes control microbial
360 assemblages. For the bacterial communities, the deterministic processes favored
361 dissimilar communities, whereas for archaeal and fungal communities, the
362 deterministic assemblage processes produced more similar communities than
363 expected by chance. However, neutral community model analysis revealed a
364 negligible degree of stochastic processes (Fig. 5b and Fig. S2), confirming its minor
365 role in the assembly of microbial communities. In addition, fungal communities
366 demonstrated wider niche breadths than the archaeal and bacterial communities (Fig.
367 5c), indicating higher fungal metabolic flexibility and redundancy. A possible
368 explanation is that the Dabaoshan mine-impacted area is a unique habitat due to
369 long-term abandonment. This As, Pb, and Zn co-contamination resulted in specific
370 environmental filtering that influences the niche breadth such as abiotic conditions,
371 biotic interactions, or geographical ranges (Malard *et al.*, 2021).

372 < Insert Fig. 5 >

373 ## 3.4 Potential metabolism and predicted functions

374 ### 3.4.1 Metal-related functions of bacterial and archaeal communities

375 The bacterial and archaeal metabolic potentials were inferred by PICRUSt2
376 analysis (Fig. S3). The obtained NSTI values for both bacterial and archaeal
377 communities were low (0.00 - 0.36; Table S6), and the mean fraction of sequences
378 used in PICRUSt2 prediction were > 99.89% (Table S6), indicating that the prediction
379 was accurate (Douglas *et al.*, 2019; Langille *et al.*, 2013). The extremely high
380 concentrations of As, Fe, Pb, and Zn in the studied tailings likely enriched the
381 abundance of metal-resistance genes during the long term (Table S1) compared to
382 short-term exposures (Liu *et al.*, 2021). Among the 6779 (for bacterial community)
383 and 3145 (for archaeal community) KOs, 23 metal-related KOs were shared for
384 bacterial and archaeal communities (Fig. S3; Table S7 and S8). Relative abundances
385 of KOs were related to arsenite transporter (K03325), arsenate reductase (K03741),
386 and Fe-S cluster assembly proteins (K09013-9015) differed between bacterial and
387 archaeal communities ($p < 0.05$; Fig. 6a).

388 < Insert Fig. 6 >

389 It was noteworthy that the detected arsenate reductase and arsenite transporter could
390 reduce As^{5+} to As^{3+} to be retained in the bacterial cell, released into the air, or both
391 (Rahman *et al.*, 2021). Although the expression of KO genes related to arsenate
392 respiratory reductase (*arr*) may not be strictly anaerobic (Jia *et al.*, 2014), the KOs
393 were not revealed by PICRUSt2 here (Fig. S3). Microorganisms harboring *arr* genes
394 can use arsenate as a terminal electron acceptor for respiration in cell periplasm
395 (Bhattacharjee and Rosen, 2000). Thus, a proportion of microorganisms should be
396 active for arsenic detoxification in the studied sites. The KOs related to Fe-S cluster

assembly protein were dominant for archaeal communities. The Fe-S cluster assembly could traffic the toxic iron and sulfide to the target metalloproteins to maintain the Fe-S homeostasis (Chahal *et al.*, 2009). The shared KOs related to Co-Zn-Cd efflux system protein (K16264) and arsenite/tail-anchored protein-transporting ATPase (K01551) were also detected (Tables S7 and S8). The arsenite/tail-anchored protein-transporting ATPase could couple with arsenic pump membrane protein for the cellular expulsion of arsenite or antimonite (Bhattacharjee and Rosen, 2000).

Additionally, specific KOs between bacterial and archaeal communities were also detected (Fig. S3 and Table S7). The distinct distribution of these predicted functional pathways was strongly correlated with As, Fe, and Pb contents (r = 0.98; Fig. 6b,c). Additional contamination, whether organic or metallic/metalloid, could modify the composition and function of microorganisms in natural habitats (Ning *et al.*, 2020; Mendez-Garcia *et al.*, 2015). For bacterial taxa, specific KOs related to the arsenate/arsenite/antimonite responsive transcriptional repressor (K03892), F-type H^+-transporting ATPase subunit *b* (K02108 - K02115), Fe^{3+} transporters (K02010, K02011, and K02012), and metal efflux systems (K15726, K07787) showed high relative abundance (Fig. S3a). The KOs related to Fe^{3+} transport and metal efflux could mediate resistance to Co^{2+}, Zn^{2+}, Cd^{2+}, and Fe^{3+} and function as a cation/proton antiport for the removal of cellular cations (Cabral *et al.*, 2016). Given the presence of several metal-efflux pumps and metal-regulated gene expression in tailings, these processes may be crucial in the detoxification of metals (Maynaud *et al.*, 2014; Ren *et al.*, 2017). For archaeal taxa, the dominant KOs related to arsenite/tail-anchored protein-transporting ATPase (K01551) were specific to the Dabaoshan As/Pb/Zn mine-impacted area (Fig. S3b and Table S8). To adapt to the extreme tailings environment, microorganisms harbored specific functions known as essential for the

biogeochemical cycling and biodegradation of pollutants (Cravo-Laureau *et al.*, 2017).

3.4.2 Functional prediction of fungal communities

We assigned fungal OTUs into specific ecological guilds based on FUNGuild (Fig. S4a). Three ecological guilds (pathogens, symbiotrophs, and saprotrophs) accounted for ~ 44.5% of all the fungal OTUs (Fig. S4a). It was surprising to detect relatively high numbers of animal pathogens and soil saprotrophs in the studied tailings (Fig. S4a). The animal pathogens always showed a high abundance in the forest or soil system with different degrees of residency: permanent, periodic, transient, and incidental (Samaddar *et al.*, 2021). The relatively high abundance of animal pathogens seen here was likely introduced anthropogenically or after surface runoff or aerial disposition. Soil saprotrophs were the key fungi in the decomposition of recalcitrant organic C, conducting biogeochemical cycles of key nutrients (Liu *et al.*, 2022c). Correlation analyses using the geochemical parameters showed that the distribution of functional fungal guilds, such as soil saprotroph was correlated with concentrations of As, Fe, and Pb ($p < 0.05$; Fig. S4c). Such observation further supports that deterministic processes are the most important process driving fungal distributions in tailings. Also, the newly updated PICRUSt2 software was utilized to explore the functional features of fungal communities (Fig. S4b). The relevant antioxidant enzymes, such as catalase, glucose-6-phosphate dehydrogenase, glutathione reductase, peroxidase, and superoxide dismutase were selected from the functional predictions (Fig. S4b and Table S9). These metal antioxidant enzymes can mitigate the membrane lipid peroxidation damage caused by metal stress, and maintain the community stability (Azevedo *et al.*, 2007; Garg and Kaur, 2013). These antioxidant enzymes could enhance the coping mechanism to metal-induced oxidative

stress in As/Pb/Zn contamination tailings. Thus, the functional fungal taxa adapting to metal stress may be potential candidates for tailings restoration. Restoration based on indigenous sulfate-reducing bacteria consortium has been applied to the maintenance and stabilization of metal(loid)s in tailings (Liu *et al.*, 2019a; Li *et al.*, 2022). Microorganisms inhabiting mine tailings require specific metabolic strategies for their survival and may hold potential resources for future pollution cleanup strategies. Effective in situ bioremediation will rely on an in-depth understanding of the function of the bacterial communities, especially the abundant and metabolically active phylotypes.

5. Conclusions

The present study provides new insight into the co-occurrence patterns of bacteria, fungi, and archaea communities in co-contaminated typical metal(loid) tailings after 20 years of abandonment. The combined mineralogy analyses revealed that As, Pb, and Zn were the major toxicants. The microbial distribution patterns indicated that the assemblages of bacterial, fungal, and archaeal taxa were influenced by the metal(loid)s (including Cu, Pb, and Sb), which suggests that deterministic processes play a key role in shaping microbial community assemblages. The microbial community arranges around keystone taxa such as members of *Mucilaginibacter*, *Cladophialophora*, and *Candidatus Nitrosotalea* genera. The PICRUSt analysis showed that specific functional KOs attested to the distinct roles of bacteria and archaea communities prevailing in the metal detoxification of tailings, such as As^{5+}. The relevant antioxidant enzymes of fungi taxa (catalase and glutathione reductase) could relieve metal-induced oxidative stress. To the best of our knowledge, the present study provides, for the first time, new insight into how microbial communities (including Bacteria, Archaea, and Fungi) respond to typical As/Pb/Zn

mine tailings. Such emerging technologies are applicable for the future restoration of soils co-contaminated with metal(loid)s from mine tailings.

Credit author statement

Jian-li Liu: Samples collecting, Data Analysis, Writing - original draft; **Jun Yao**: Writing-Reviewing and Editing, and Validation; **Ruofei Li**: Samples collecting; **Houquan Liu** and **Jun-jie Zhu**: Morphological analysis of main mineral grains; **Geoffrey Sunahara** and **Robert Duran**: Writing - Review & Editing.

Declaration of competing interest

The authors declare that no conflict of financial interest or personal relationships exists in the submission of this manuscript.

Data availability

Data will be made available on request.

Acknowledgments

This work is supported in part by grants from projects of the Major National R & D Projects For the Chinese Ministry of Science and Technology (2020YFC1807600), and the National Natural Science Foundation of China (42007289), the 111 Project (B21017), the 1000-Talents Plan Project (WQ2017110423), and the Fundamental Research Funds for the Central Universities (53200759777).

Appendix A. Supporting information

Supplementary data related to this article can be found on the website of ***Science of the Total Environment***.

References

Alakangas L., Ohlander B., Lundberg A., 2010. Estimation of temporal changes in oxidation rates of sulphides in copper mine tailings at Laver, Northern Sweden. *Sci. Total Environ.* 408, 1386-1392. https://doi.org/10.1016/j.scitotenv.2009.11.005

Azevedo M.M., Carvalho A., Pascoal C., Rodrigues F., Cássio F., 2007. Responses of antioxidant defenses to Cu and Zn stress in two aquatic fungi. *Sci Total Environ.* 377(2-3), 233-43. https://doi.org/10.1016/j.scitotenv.2007.02.027

Banerjee S., Schlaeppi K., van der Heijden, M.G.A., 2018. Keystone taxa as drivers of microbiome structure and functioning. *Nat. Rev. Microbiol.* 16, 567-576. https://doi.org/10.1038/s41579-018-0024-1

Bao Y., Guo C., Lu G., Yi X., Wang H., Dang Z., 2018. Role of microbial activity in Fe(III) hydroxysulfate mineral transformations in an acid mine drainage-impacted site from the Dabaoshan Mine. *Sci Total Environ.* 616-617, 647-657. https://doi.org/10.1016/j.scitotenv.2017.10.273

Bhattacharjee H., Rosen B.P., 2000. Role of conserved histidine residues in metalloactivation of the *ArsA* ATPase. *Biometals* 13, 281-288. https://doi.org/10.1023/a:1009200215328

Brochier-Armanet C., Boussau B., Gribaldo S. Forterre P., 2008. Mesophilic crenarchaeota: Proposal for a third archaeal phylum, the *Thaumarchaeota*. *Nat. Rev. Microbiol.* 6, 245-252. https://doi.org/10.1038/nrmicro1852

Bruneel O., Pascault N., Egal M., Bancon-Montigny C., Goni-Urriza M.S., Elbaz-Poulichet F., Personné J.-C., Duran R., 2008. Archaeal diversity in a Fe-As rich acid mine drainage at Carnoules (France). *Extremophiles* 12, 563-571. https://doi.org/10.1007/s00792-008-0160-z

Cabral L., Júnior G.V.L., Pereira De Sousa S.T., Franco Dias A.C., Cadete L.L., Dini Andreote F., Hess M., de Oliveira V.M., 2016. Anthropogenic impact on mangrove sediments triggers differential responses in the heavy metals and antibiotic resistomes of microbial communities. *Environ. Pollut.* 216, 460-469. https://doi.org/10.1016/j.envpol.2016.05.078

Chahal H.K., Dai Y., Saini A., Ayala-Castro C., Outten F.W., 2009. The *SufBCD* Fe-S scaffold complex interacts with *SufA* for Fe-S cluster transfer. *Biochemistry* 48, 10644-10653. https://doi.org/10.1021/bi901518y

Chen Y.T., Li J.T., Chen L.X., Hua Z.S., Huang L.N., Liu J., Xu B.B., Liao B., Shu W.S., 2014. Biogeochemical processes governing natural pyrite oxidation and release of acid

metalliferous drainage. *Environ. Sci. Technol.* 48, 5537-5545. https://doi.org/10.1021/es500154z

Chen Z., Liu W., Zhong X., Fei Y., He H., Ding K., Chao Y., Tang Y.,Wang S., Qiu R., 2021. Genome- and community-level interaction insights into the ecological role of archaea in rare earth element mine drainage in South China. *Water Res.* 201, 117331. https://doi.org/10.1016/j.watres.2021.117331

Cravo-Laureau C., Cagnon C., Lauga B., Duran R., 2017. Microbial Ecotoxicology. Springer International Publishing, Switzerland. https://doi.org/10.3389/fmicb.2020.01342

Douglas G.M., Maffei V.J., Zaneveld J., Yurgel S.N., Brown J.R., Taylor C.M., Huttenhower C., Langille M.G.I., 2019. PICRUSt2: an improved and extensible approach for metagenome inference. *bioRxiv* http://dx.doi.org/10.1101/672295

Frenk S., Hadar Y., Minz D., 2018. Quality of irrigation water affects soil functionality and bacterial community stability in response to heat disturbance. *Appl. Environ. Microbiol.* 84, e02087-17. https://doi.org/10.1128/AEM.02087-17

Garg N. and Kaur H., 2013. Response of antioxidant enzymes, phytochelatins and glutathione production towards Cd and Zn stresses in *Cajanus cajan* (L.) Millsp. genotypes colonized by arbuscular mycorrhizal fungi. *J. Agron. Crop Sci.* 199, 118-133. https://doi.org/10.1111/j.1439-037X.2012.00533.x

Giloteaux L., Duran R., Casiot C., Bruneel O., Elbaz-Poulichet F.,Goñi-Urriza M., 2013. Three-year survey of sulfate-reducing bacteria community structure in Carnoulès acid mine drainage (France), highly contaminated by arsenic. *FEMS Microbiol. Ecol.* 83,724-737. https://doi.org/10.1111/1574-6941.12028

Han Y., Wang J., Zhao Z, Chen J., Lu H., Liu G., 2017. Fishmeal application induces antibiotic resistance gene propagation in mariculture sediment. *Environ. Sci. Technol.* 51, 10850-10860. https://doi.org/10.1021/acs.est.7b02875

Herren C.M. and McMahon K.D., 2018. Keystone taxa predict compositional change in microbial communities. *Environ Microbiol.* 20, 2207-2217. https://doi.org/10.1111/1462-2920.14257

Hudson-Edwards K., 2016. Tackling mine wastes. *Science* 352, 288-290. http://doi.org/10.1126/science.aaf3354

Hugoni M., Taib N., Debroas D., Domaizon I., Dufournel I.J., Bronner G., Salter I., Agogué H., Mary I., Galand P.E., 2013. Structure of the rare archaeal biosphere and seasonal dynamics of active ecotypes in surface coastal waters. *PNAS* 110, 6004-6009.

https://doi.org/10.1073/pnas.1216863110

Jia T., Wang X., Guo T., Chai B., 2021. Litter decomposition of *Imperata cylindrica* in a copper tailing areas with different restoration history: Fungal community dynamics and driving factors. *Front. Microbiol.* 12, 780015. https://doi.org/10.3389/fmicb.2021.780015

Jia Y., Huang H., Chen Z., Zhu Y., 2014. Arsenic uptake by rice is influenced by microbe-mediated arsenic redox changes in the rhizosphere. *Environ. Sci. Technol.* 48, 1001-1007. https://doi.org/10.1021/es403877s

Langille M.G.I., Zaneveld J., Caporaso J.G., McDonald D., Knights D., Reyes J.A., Clemente J.C., Burkepile D.E., Vega Thurber R.L., Knight R., Beiko R.G., Huttenhower C., 2013. Predictive functional profiling of microbial communities using 16S rRNA marker gene sequences. *Nat. Biotechnol.* 31, 814-821. https://doi.org/10.1038/nbt.2676

Latzel V., Allan E., Bortolini S.A., Colot V., Fischer M., Bossdorf O., 2013. Epigenetic diversity increases the productivity and stability of plant populations. *Nat. Commun.* 4, 2875. https://doi.org/10.1038/ncomms3875

Lehtovirta-Morley L.E., Sayavedra-Soto L.A., Gallois N., Schouten S., Stein L.Y., Prosser J.I., Nicola G.W., 2016. Identifying potential mechanisms enabling acidophily in the ammonia-oxidizing archaeon "*Candidatus Nitrosotalea devanaterra.*" *Appl Environ Microbiol.* 82, 2608-2619. https://doi.org/10.1128/aem.04031-15

Liang J., Liu J., Jia P., Yang T., Zeng Q., Zhang S., Liao B., Shu W., Li J., 2020. Novel phosphate-solubilizing bacteria enhance soil phosphorus cycling following ecological restoration of land degraded by mining. *ISME J.* 14, 1600-1613. https://doi.org/10.1038/s41396-020-0632-4

Li M., Yao J., Sunahara G., Hawari J., Duran R., Liu J., Liu B., Cao Y., Pang W., Li H., Li Y., Ruan Z., 2022. Novel microbial consortia facilitate metalliferous immobilization in non-ferrous metal(loid)s contaminated smelter soil: efficiency and mechanisms. *Environ Pollut.* 15, 120042. https://doi.org/10.1016/j.envpol.2022.120042

Liu B., Yao J., Chen Z., Ma B., Liu J., Li H., Zhu X., Li M., Cao Y., Pang W., Zhao C., Mihucz V.G., Duran R., 2022a. Unraveling ecological risk of As/Sb and other metal(loid)s and fungal community responses in As/Sb smelting-intensive zone: A typical case study of Southwest China. *J. Clean. Prod.* 338, 130525. https://doi.org/10.1016/j.jclepro.2022.130525

Liu B., Yao J., Ma B., Li S., Duran R., 2022b. Disentangling biogeographic and underlying assembly patterns of fungal communities in metalliferous mining and smelting soils. *Sci.*

598 *Total Environ.* 845, 157151. https://doi.org/10.1016/j.scitotenv.2022.157151

599 Liu J., Yao J., Duran R., Mihucz V.G., Hudson-Edwards K.A., 2019a. Bacterial shifts during
600 in-situ mineralization bio-treatment to non-ferrous metal(loid) tailings. *Environ. Pollut.*
601 255, 113165. https://doi.org/10.1016/j.envpol.2019.113165

602 Liu J., Yao J., Wang F., Ni W., Liu X., Sunahara G., Duran R., Jordan G., Hudson-Edwards
603 K.A., Alakangas L., Solevic-Knudsen T., Zhu X., Zhang Y., Li Z., 2018. China's most
604 typical nonferrous organic-metal facilities own specific microbial communities. *Sci.*
605 *Rep-UK* 8, 12570-12580. https://doi.org/10.1038/s41598-018-30519-1

606 Liu J., Yao J., Wang F., Min N., Gu J., Li Z., Sunahara G., Duran R., Solevic-Knudsen T.,
607 Hudson-Edwards K.A., Alakangas L., 2019b. Bacterial diversity in typical abandoned
608 multi-contaminated nonferrous metal(loid) tailings during natural attenuation. *Environ.*
609 *Pollut.* 247, 98-107. https://doi.org/10.1016/j.envpol.2018.12.045

610 Liu J., Yao J., Zhou D., Liu B., Liu H., Li M., Zhao C., Sunahara G., Duran R., 2023.
611 Mining-related multi-resistance genes in sulfate-reducing bacteria treatment of typical
612 karst nonferrous metal(loid) mine tailings in China. *Environ. Sci. Pollut. R.* 30,
613 104753-104766. https://doi.org/10.1007/s11356-023-29203-3

614 Liu J., Yao J., Zhu X., Zhou D., Duran R., Mihucz V.G., Bashir S., Hudson-Edwards K.A.,
615 2021. Metagenomic exploration of multi-resistance genes linked to microbial attributes
616 in active nonferrous metal(loid) tailings. *Environ. Pollut.* 273, 115667.
617 https://doi.org/10.1016/j.envpol.2020.115667

618 Liu S., García-Palacios P., Tedersoo L., Guirado E., van der Heijden M.G.A., Wagg C., Chen
619 D., Wang Q., Wang J., Singh B.K., Delgado-Baquerizo M., 2022c. Phylotype diversity
620 within soil fungal functional groups drives ecosystem stability. *Nat. Ecol. Evol.* 6,
621 900-909. https://doi.org/10.1038/s41559-022-01756-5

622 Lloyd C., 2023. Cultured microbial diversity of Parys mountain acidic site. PhD thesis.
623 School of Environmental and Natural Sciences, UK: Bangor University.

624 Luo C., Routh J., Luo D., Wei L., Liu Y., 2021. Arsenic in the Pearl River Delta and its
625 related waterbody, South China: occurrence and sources, a review. *Geosci. Lett.* 8, 12.
626 https://doi.org/10.1186/s40562-021-00185-9

627 Malard L.A., Mod H.K., Guex N., Broennimann O., Yashiro E., Lara E., Mitchell E.A.,
628 Niculita-Hirzel H., Guisan A., 2021. Comparative analysis of diversity and
629 environmental niches of soil bacterial, archaeal, fungal and protist communities reveal
630 niche divergences along environmental gradients in the Alps. *Soil Biol. Biochem.* 169,
631 108674. https://doi.org/10.1016/j.soilbio.2022.108674

632 Mamet S.D., Lamb E.G., Piper C.L., Winsley T., Siciliano S.D., 2017. Archaea and bacteria
633 mediate the effects of native species root loss on fungi during plant invasion. *ISME J.* 11,
634 1261-1275. https://doi.org/10.1038/ismej.2016.205

635 Maynaud G., Brunel B., Yashiro E., Mergeay M., Cleyet-Marel J.C., Le Quéré A., 2014.
636 *CadA* of *Mesorhizobium metallidurans* isolated from a zinc-rich mining soil is a
637 P(IB-2)-type ATPase involved in cadmium and zinc resistance. *Res Microbiol.* 165,
638 175-89. https://doi.org/10.1016/j.resmic.2014.02.001

639 Mendez-Garcia C., Pelaez A. I., Mesa V., Sánchez J., Golyshina O.V., Ferrer M., 2015.
640 Microbial diversity and metabolic networks in acid mine drainage habitats. *Front.*
641 *Microbiol.* 6, 475. https://doi.org/10.3389/fmicb.2015.00475

642 Moussa T.A.A., Al-Zahrani H.S., Almaghrabi O.A., Abdelmoneim T.S., Fuller M.P., 2017.
643 Comparative metagenomics approaches to characterize the soil fungal communities of
644 western coastal region, Saudi Arabia. *PLOS ONE* 12, e0185096.
645 https://doi.org/10.1371/journal.pone.0185096

646 Nguyen N.H., Song Z., Bates S.T., Branco S., Tedersoo L., Menke J., Schilling J.S., Kennedy
647 P.G., 2016. FUNGuild: an open annotation tool for parsing fungal community datasets
648 by ecological guild. *Fungal Ecol.* 20, 241-248.
649 https://doi.org/10.1016/j.funeco.2015.06.006

650 Ning D., Yuan M., Wu L., Zhang Y., Guo X., Zhou X., Yang Y., Arkin A.P., Firestone M.K.,
651 Zhou J., 2020. A quantitative framework reveals ecological drivers of grassland
652 microbial community assembly in response to warming. *Nat. Commun.* 11, 4717.
653 https://doi.org/10.1038/s41467-020-18560-z

654 Rahman M.S., Hossain M.S., Saha S.K., Rahman S., Sonne C., Kim K., 2021. Homology
655 modeling and probable active site cavity prediction of uncharacterized arsenate reductase
656 in bacterial spp. *Appl. Biochem. Biotechnol.* 193, 3119-3135.
657 https://doi.org/10.1007/s12010-020-03392-w

658 Ren S., Li Q., Xie L., Xie J., 2017. Molecular mechanisms underlying the function diversity
659 of *ArsR* family metalloregulator. *Crit. Rev. Eukar. Gene.* 27, 19-35.
660 https://doi.org/10.1615/critreveukaryotgeneexpr.2016018476

661 Samaddar S., Karp D. S., Schmidt R., Devarajan N., McGarvey J.A., Pires A.F.A., Scow K.,
662 2021. Role of soil in the regulation of human and plant pathogens: soils' contributions to
663 people. *Phil. Trans. R. Soc. B* 376, 20200179. https://doi.org/10.1098/rstb.2020.0179

664 Sheridan P.O., Meng Y., Williams T.A., Gubry-Rangin C., 2022. Recovery of
665 *Lutacidiplasmatales* archaeal order genomes suggests convergent evolution in

Thermoplasmatota. *Nat. Commun* 13, 4110. https://doi.org/10.1038/s41467-022-31847-7

Sloan W.T., Lunn M., Woodcock S., Head I.M., Nee S., Curtis T.P., 2006. Quantifying the roles of immigration and chance in shaping prokaryote community structure. *Environ. Microbiol.* 8, 732-740. https://doi.org/10.1111/j.1462-2920.2005.00956.x

Speer R.M., Zhou X., Volk L.B., Liu K.J., Hudson L.G., 2023. Arsenic and cancer: Evidence and mechanisms. *Adv. Pharmacol.* 96, 151-202. https://doi.org/10.1016/bs.apha.2022.08.001

Sun W., Xiao E., Haggblom M., Krumins V., Dong Y., Sun X., Li F., Wang Q., Li B., Yan B., 2018. Bacterial survival strategies in an alkaline tailing site and the physiological mechanisms of dominant phylotypes as revealed by metagenomic analyses. *Environ. Sci. Technol.* 52, 13370-13380. https://doi.org/10.1021/acs.est.8b03853

Sunagawa S., Coelho L. P., Chaffron S. *et al*., 2015. Structure and function of the global ocean microbiome. *Science* 348, 6237. https://hal.science/hal-01233742

Suting E.G. and Olivia Devi N., 2021. Occurrence and diversity of arbuscular mycorrhizal fungi in trap cultures from limestone mining sites and un-mined forest soil of Mawsmai, Meghalaya. *Trop. Ecol.* 62, 525-537. https://doi.org/10.1007/s42965-021-00144-7

Taleski V., Dimkić I., Boev B., Boev I., Živković S., Stanković S., 2020. Bacterial and fungal diversity in the lorandite (TlAsS2) mine 'Allchar' in the Republic of North Macedonia. *FEMS Microbiol.* Ecol. 96, 155. https://doi.org/10.1093/femsec/fiaa155

Torres S.B., Petrik A., Szabo K.Z., Jordan G., Yao J., Szabó C., 2018. Spatial relationship between the field-measured ambient gamma dose equivalent rate and geological conditions in a granitic area, Velence Hills, Hungary: an application of digital spatial analysis methods. *J. Environ. Radioactiv.* 192, 267-278. https://doi.org/10.1016/j.jenvrad.2018.07.001

Tuhý M., Hrstka T., Ettler V., 2020. Automated mineralogy for quantification and partitioning of metal(loid)s in particulates from mining/smelting-polluted soils. *Environ. Pollut.* 266, 115118. https://doi.org/10.1016/j.envpol.2020.115118

Umezawa K., Kojima H., Kato Y., Fukui M., 2020. Disproportionation of inorganic sulfur compounds by a novel autotrophic bacterium belonging to *Nitrospirota*. *Syst. Appl. Microbiol.* 43, 126110. https://doi.org/10.1016/j.syapm.2020.126110

Vasconcelos A.L.S., Defalco T., Dias A.C.F., Barrientos L., Bernardino A.F., Andreote F.D., Núñez-Montero K., 2021. Complete genome sequence of a *Mucilaginibacter* sp. strain isolated from estuarine soil contaminated with mine tailings from the Samarco Disaster

699 at Fundão Dam. *Microbiol. Resour. Announc.* 10, e0077921.
700 https://doi.org/10.1128/mra.00779-21

701 Wang L., Ji B., Hu Y., Liu R., Sun W., 2017. A review on in situ phytoremediation of mine
702 tailings. *Chemosphere* 184, 594-600. https://doi.org/10.1016/j.chemosphere.2017.06.025

703 Wang Y., Dong R., Zhou Y., Luo X., 2019. Characteristics of groundwater discharge to river
704 and related heavy metal transportation in a mountain mining area of Dabaoshan,
705 Southern China. *Sci. Total Environ.* 679, 346-358.
706 https://doi.org/10.1016/j.scitotenv.2019.04.273

707 Xiao E., Krumins V., Dong Y., Xiao T., Ning Z., Xiao Q., Sun W., 2016. Microbial diversity
708 and community structure in an antimony-rich tailings dump. *Appl. Microbiol. Biotechnol.*
709 100, 7751-7763. https://doi.org/10.1007/s00253-016-7598-1

710 Yi X.Y., Yang Y.P., Yuan H.Y., Chen Z., Suan G., Zhu Y., 2019. Coupling metabolisms of
711 arsenic and iron with humic substances through microorganisms in paddy soil. *J. Hazard.*
712 *Mater.* 373, 591-599. https://doi.org/10.1016/j.jhazmat.2019.03.113

713 Yi X., Liang J., Su J., Jia P., Lu J., Zheng J., Wang Z., Feng S., Luo Z., Ai H., Liao B., Shu
714 W., Li J., Zhu Y., 2022. Globally distributed mining-impacted environments are
715 underexplored hotspots of multidrug resistance genes. *ISME J.* 16, 2099-2113.
716 https://doi.org/10.1038/s41396-022-01258-z

717 Zhang Y., Wang F., Hudson-Edwards K., Blake R., Zhao F., Yuan Z., Gao W., 2020.
718 Characterization of mining-related aromatic contaminants in active and abandoned
719 metal(loid) tailings ponds. *Environ. Sci. Technol.* 54, 15097-15107.
720 https://doi.org/10.1021/acs.est.0c03368

721 Zhu X., Yao J., Wang F., Yuan Z., Liu J., Jordan G., Šolević Knudsen T., Avdalović J., 2018.
722 Combined effects of antimony and sodium diethyldithiocarbamate on soil microbial
723 activity and speciation change of heavy metals. Implications for contaminated lands
724 hazardous material pollution in nonferrous metal mining areas. *J. Hazard. Mater.* 349,
725 160-167. https://doi.org/10.1016/j.jhazmat.2018.01.044

726 Zhu J., Yang K., Chen Y., Fan G., Zhang L., 2021. Revealing the substitution preference of
727 zinc in ordinary Portland cement clinker phases: a study from experiments and DFT
728 calculations. *J. Hazard. Mater.* 409, 124504.
729 https://doi.org/10.1016/j.jhazmat.2020.124504

Figure legends

Fig. 1 SEM images of collected tailings samples, and XRD analysis of collected tailings samples. a: Quartz (PDF# 46-1045), b: Manganese copper oxide (PDF# 82-0668), c: Iwakiite (PDF# 38-0430), d: Celadonite (PDF# 17-0521), e: Magnesium iron oxide (PDF# 77-2367).

Fig. 2 General patterns of microbial alpha-diversity and community assembly. (a) Alpha-diversity of bacterial, fungal, and archaeal in the sampling sites. Significant difference (based on the Wilcoxon test; $p \leq 0.05$). Relative abundance of (b) bacterial, (c) fungal, and (d)archaeal communities. Bubble sizes represent the relative abundance of the genera. The bubble color is colored according to the classification information.

Fig. 3 General patterns of microbial beta-diversity in studied tailings. (a-d) Respective beta-diversity of bacterial, fungal, archaeal, and all taxa communities based on non-metric multidimensional scaling (NMDS) analysis. (e) Partial Mantel test for co-relation of three microbial groups and physical-chemical parameters. A color gradient denotes the Pearson's correlation coefficients.

Fig. 4 Metacommunity network analysis for the detected bacterial, fungal, and archaeal taxa in tailings. Each node indicates one OTU. The corresponding species of each OTU was listed in Table S6. The colors of the node represent the different major phyla and genera. The size of the species-node denotes the abundance of species. Nodes unnamed represented the no_rank/un-classified genera. The red line represents the positive correlation between the two individual nodes, and the green line shows a negative (exclusion) correlation.

Fig. 5 (a) Variation of incidence-based (Raup-Crick) beta-diversity for microbial communities. (b) Comparison of the maximum likelihood fit of the neutral models estimated by the Akaike information criterion for microbial communities in tailings. (c) Comparison of mean habitat niche breadths in all taxa in bacterial, fungal, and archaeal communities.

Fig. 6 Independent-samples *T*-test and correlation of KOs with geochemical parameters. (a) Difference analysis for KOs related to metals of bacterial and archaeal communities based on the independent-sample *T*-test. Data for the 23 shared KOs were used for analysis. *$0.01 < p \leq 0.05$, **$0.001 < p \leq 0.01$, *** $p \leq 0.001$. (b and c) Redundancy analyses (RDA) of geochemical parameters (arrows) and KEGG pathways (*) of bacterial and archaeal communities, respectively.

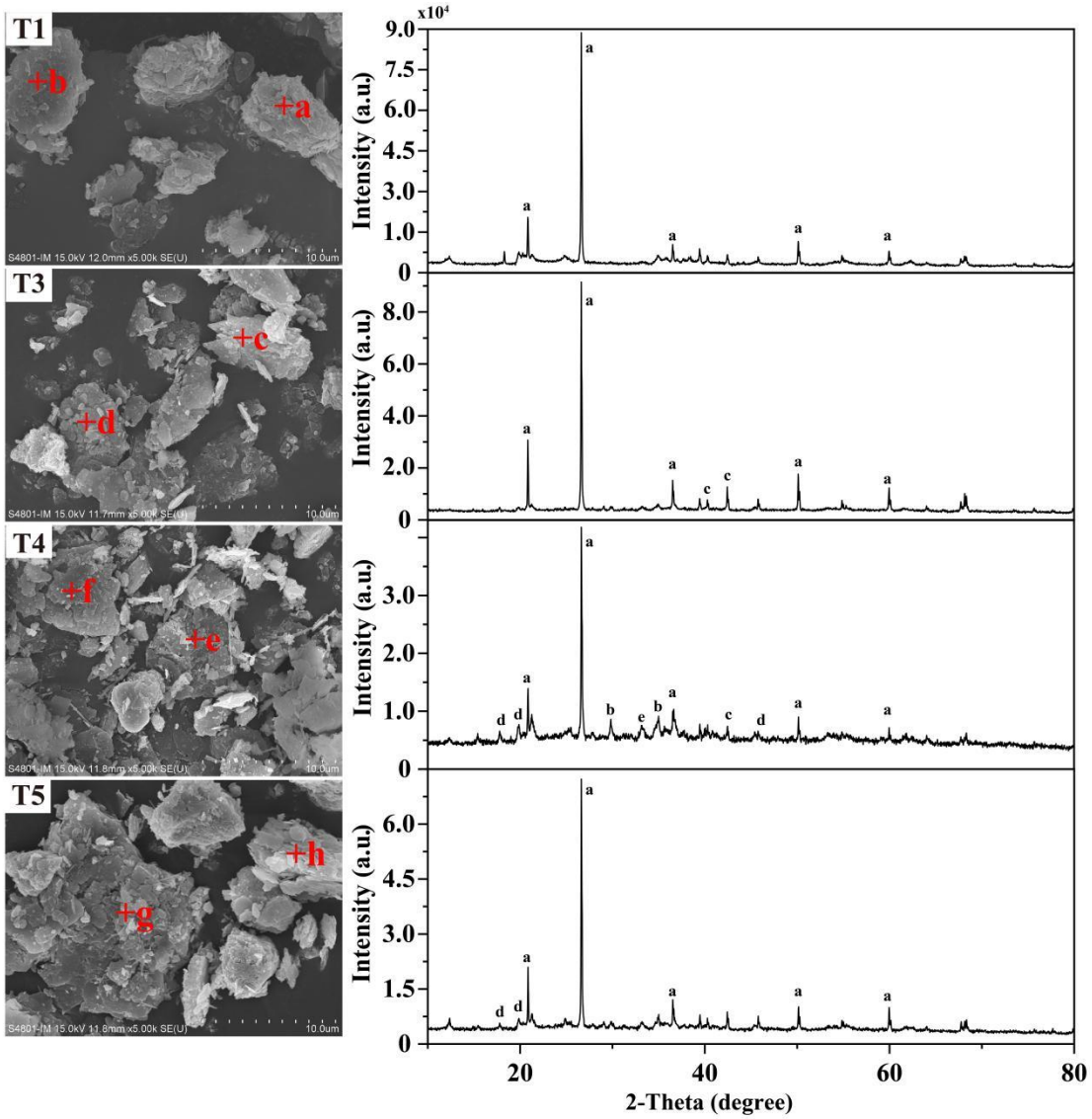

Fig. 1 SEM images of collected tailings samples, and XRD analysis of collected tailings samples. a: Quartz (PDF# 46-1045), b: Manganese copper oxide (PDF# 82-0668), c: Iwakiite (PDF# 38-0430), d: Celadonite (PDF# 17-0521), e: Magnesium iron oxide (PDF# 77-2367).

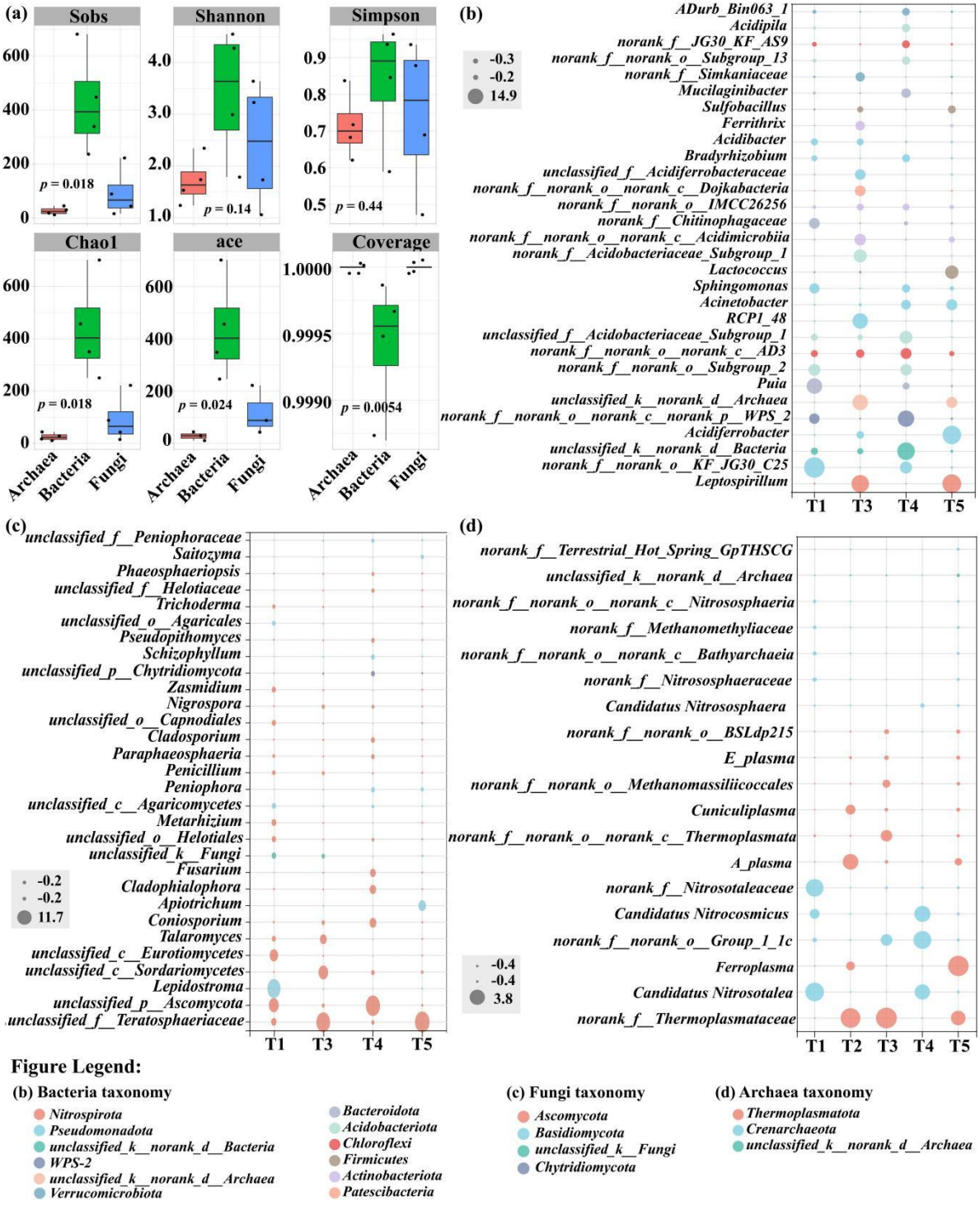

Fig. 2 General patterns of microbial alpha-diversity and community assembly. (a) Alpha-diversity of bacterial, fungal, and archaeal in the sampling sites. Significant difference: $p \leq 0.05$ (analysis was based on the Wilcoxon test). (b-d) Relative abundance of microorganisms, corresponding to bacterial, fungal, and archaeal communities, respectively. Bubble size represented the relative abundance of the genus. The bubble color indicates the classification information.

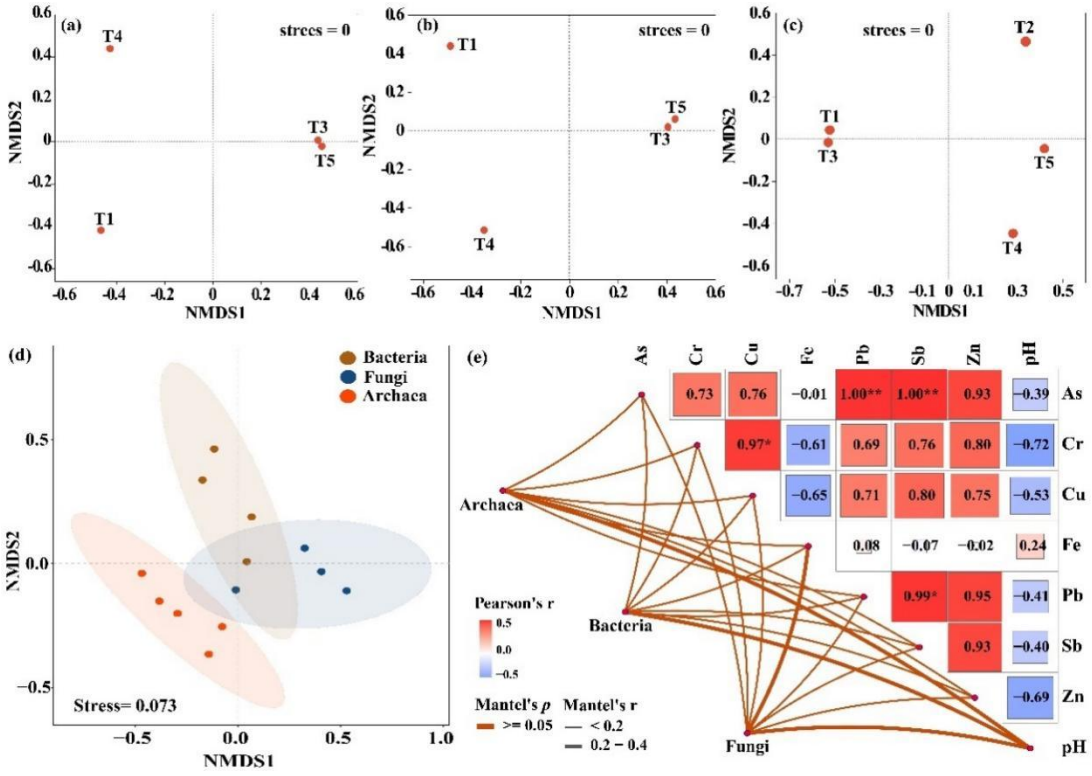

Fig. 3 General patterns of microbial beta-diversity in studied tailings. (a-d) Beta-diversity of bacterial, fungal, archaeal, and all taxa communities based on non-metric multidimensional scaling (NMDS) analysis. (e) Partial Mantel test for correlation of three microbial groups and physical-chemical parameters. A color gradient denotes the Pearson's correlation coefficients.

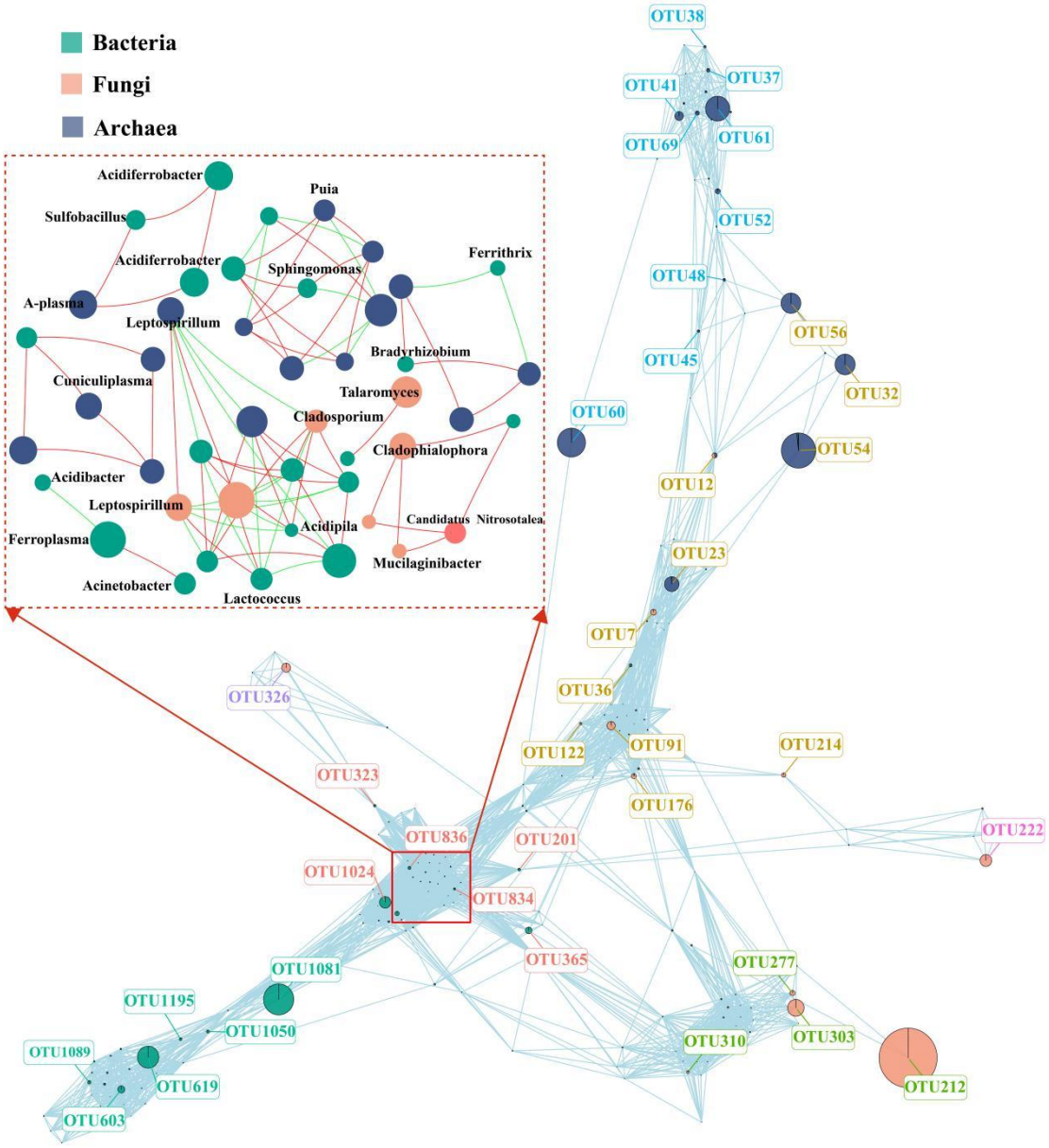

Fig. 4 Metacommunity network analysis for the detected bacterial, fungal, and archaeal taxa in tailings. Each node indicates one OTU. The corresponding species of each OTU was listed in Table S6. The colors of the nodes represent the different major phyla and genera. The size of the species-node denotes the abundance of species. Nodes unnamed represented the no_rank/un-classified genera. The red lines represent the positive correlations between the two individual nodes, the green lines show negative (exclusion) correlations.

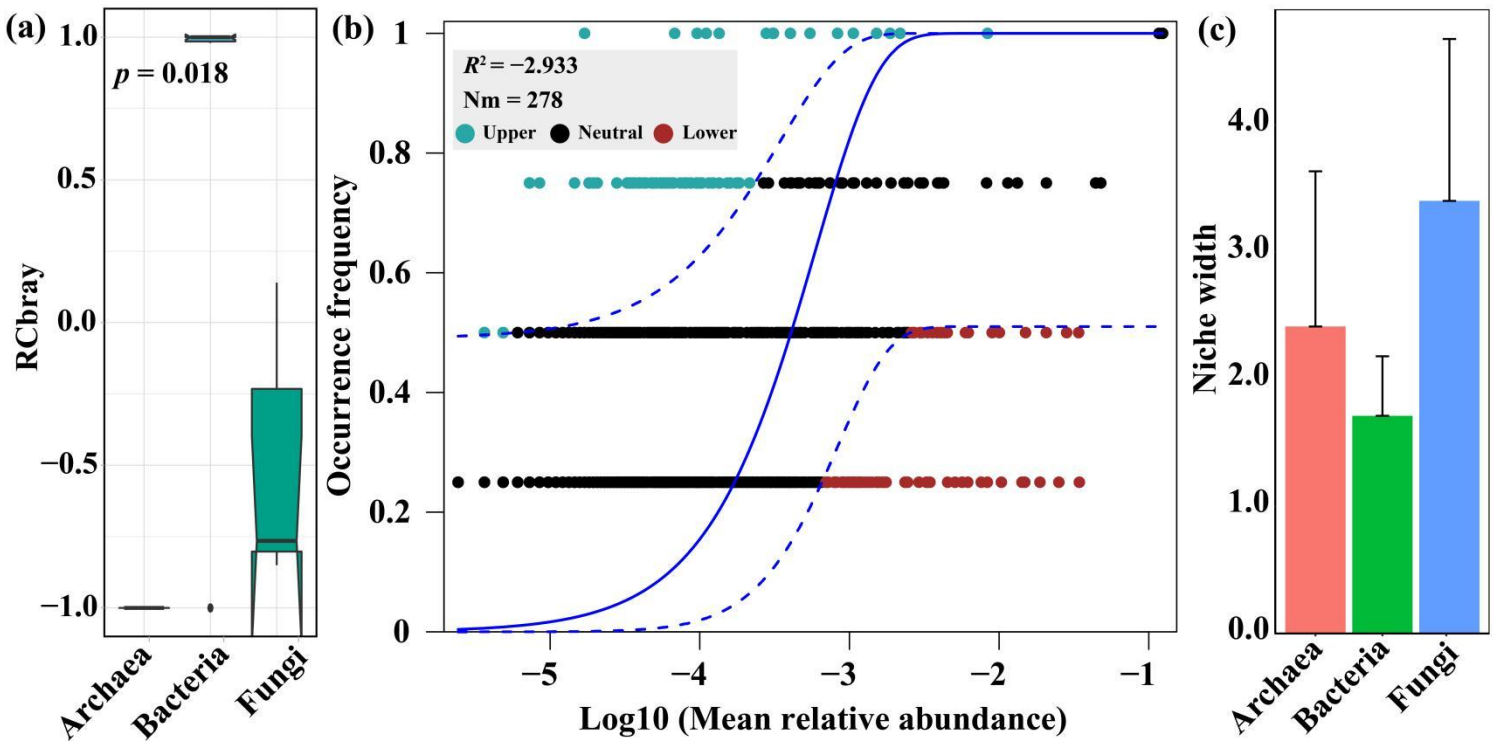

Fig. 5 (a) Variation of incidence-based (Raup-Crick) beta-diversity for microbial communities. (b) Comparison of the maximum likelihood fit of the neutral models estimated by the Akaike information criterion for microbial communities in tailings. (c) Comparison of mean habitat niche breadths in all taxa in bacterial, fungal, and archaeal communities.

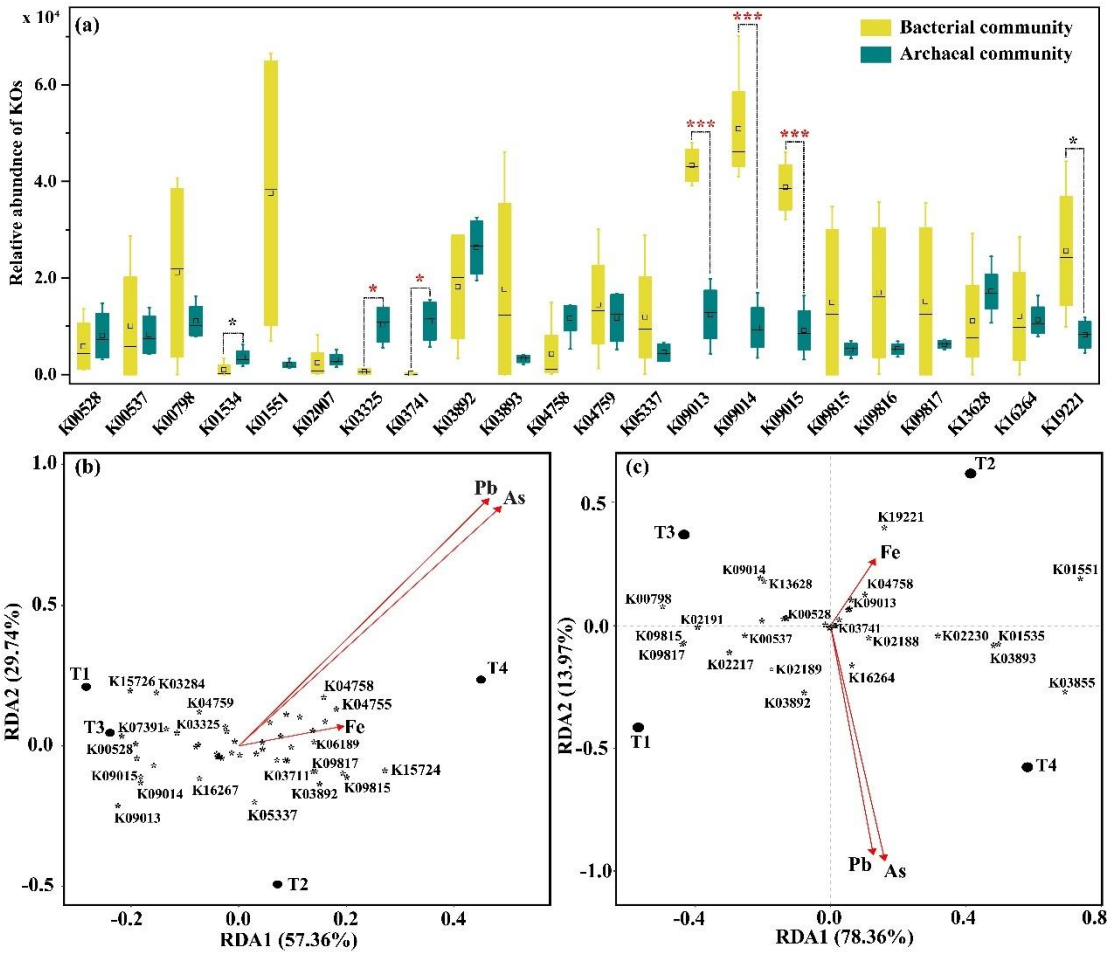

Fig. 6 Independent-sample *T*-tests and correlations of KOs with geochemical parameters. (a) Difference analysis for KOs related to metals of bacterial and archaeal communities based on the independent-sample *T*-test. Data for the 23 shared KOs were used for analysis. *$0.01 < p \leq 0.05$, **$0.001 < p \leq 0.01$, *** $p \leq 0.001$. (b and c) Redundancy analysis (RDA) of geochemical parameters (arrows) and KEGG pathways (*) of bacterial and archaeal communities, respectively.